

Thermal Behavior and Crystal Structure of Dichloro[6-amino-1,3-dimethyl-5-(2-chlorophenylazo)uracilato]gold(III)

ENRIQUE COLACIO RODRÍGUEZ, JOSÉ RUIZ SÁNCHEZ, JUAN DE DIOS LÓPEZ GONZÁLEZ, JUAN MANUEL SALAS PEREGRÍN*

Departamento de Química Inorgánica, Facultad de Ciencias, Universidad de Granada, 18071 Granada (Spain)

MARC J. OLIVIER, MIGUEL QUIRÓS and ANDRÉ L. BEAUCHAMP*

Département de Chimie, Université de Montréal, C.P. 6128, Succ. A, Montréal, Que., H3C 3J7 (Canada)

(Received October 16, 1989)

Abstract

The title compound was obtained by reacting HAuCl_4 with the uracil derivative in ethanol. X-ray work ($P2_1/c$, $a = 11.896(6)$, $b = 12.331(5)$, $c = 13.501(4)$ Å, $\beta = 121.46(3)^\circ$, $R = 0.038$, 2096 observed reflections) shows that the crystal contains individual complex molecules in which the metal has a slightly distorted square-planar coordination. Two *cis* corners are occupied by Cl ligands. The uracil derivative forms a six-membered chelate ring via the deprotonated amino group and the phenyl-substituted nitrogen atom of the azo group. The thermal behavior of the free ligand and its Au complex has been determined from thermogravimetric and differential scanning calorimetric measurements.

Introduction

During the past few years, important biological and medical applications have been uncovered for gold compounds, creating increasing interest in the coordination chemistry of this element. For example, some of its complexes have been reported to possess antitumor properties [1–3], whereas the activity of the gold(I) compounds myocrisin and auronofin as injectable and orally-absorbed antiarthritic drugs is well documented [4–8]. Nevertheless, the chemistry of Au(III) is much less developed than that of the iso-electronic and often isostructural Pt(II) atom. The interaction of gold compounds with nitrogen ligands has received relatively little attention, in spite of the interest of such compounds as potential anticancer agents.

As part of our research program on the reactions of metal ions with various ligands derived from pyrimidine, we wish to report on a complex isolated

by reacting HAuCl_4 with 6-amino-1,3-dimethyl-5-(2-chlorophenylazo)uracil, a ligand interesting in its own right because of the presence of an arylazo group providing antineoplastic activity [9]. Crystallographic work on gold compounds with ligands of this type has been restricted so far to our previous work on salts containing the protonated cation without direct Au–ligand bonding [7, 10]. The only other crystallographically characterized Au(III) complex with a pyrimidine derivative is the N3-bonded compound with 1-methylcytosine [11].

Experimental

Preparation of 6-Amino-1,3-dimethyl-5-(2-chlorophenylazo)uracil (DZCH)

o-Chloroaminobenzene (0.05 mol) was mixed with 23.5 ml of 1.75 M aqueous HCl. The mixture was cooled to 5 °C, and 0.05 mol of NaNO_2 was added to obtain the corresponding yellow diazonium salt. To the suspension of this salt was added a solution of 6-amino-1,3-dimethyluracil (0.05 mol) [12] in 50 ml of water. A yellow precipitate formed immediately. After the reaction mixture was stirred for 1 h at 5 °C, the yellow precipitate was collected by filtration, washed with cold water, and air dried. It was recrystallized from pyridine to yield yellow needles. *Anal.* Calc. for $\text{C}_{12}\text{H}_{12}\text{ClN}_5\text{O}_2$: C, 49.06; H, 4.12; N, 23.84. Found: C, 48.62; H, 4.11; N, 23.58%.

Preparation of Dichloro[6-amino-1,3-dimethyl-5-(2-chlorophenylazo)uracilato]gold(III), [Au(DZC)Cl₂]

A mixture of DZCH (0.85 mmol, 0.29 g) and HAuCl_4 (0.85 mmol, 0.32 g) in ethanol was refluxed for 1 h and allowed to cool to room temperature. The red precipitate was filtered off and air dried. *Anal.* Calc. for $\text{C}_{12}\text{H}_{11}\text{AuCl}_3\text{N}_5\text{O}_2$: C, 25.71; H, 1.98; N, 12.49; Au, 35.15. Found: C, 25.97; H, 2.07; N, 12.47; Au, 34.93%.

* Authors to whom correspondence should be addressed.

Instruments and Techniques

Infrared spectra were recorded on a Perkin-Elmer 983G spectrophotometer on KBr discs (4000–200 cm^{-1}) or polyethylene pellets (600–180 cm^{-1}). C, H, N microanalyses were performed by the Micro-analytical Laboratory of the Bioorganic Institute C.S.I.C., Barcelona. Au was determined gravimetrically as the metal.

Thermogravimetric studies were performed at a heating rate of 10 $^{\circ}\text{C min}^{-1}$ and with a dynamic atmosphere (100 ml min^{-1}) of pure air, by using a Mettler TG-50 thermobalance and a Mettler DSC-20 differential scanning calorimeter.

Crystallographic Work

$\text{C}_{12}\text{H}_{11}\text{AuCl}_3\text{N}_5\text{O}_2$, $FW = 560.6$, monoclinic, space group $P2_1/c$, $a = 11.896(6)$, $b = 12.331(5)$, $c = 13.501(4)$ \AA , $\beta = 121.46(3)^{\circ}$, $V = 1689.5$ \AA^3 , $D_c = 2.203$ g cm^{-3} , $Z = 4$, $F(000) = 1056$, $\lambda(\text{Mo K}\alpha) = 0.71069$ \AA (graphite monochromator), $\mu(\text{Mo K}\alpha) = 91.71$ cm^{-1} , $T = 293$ K, crystal dimensions (faces): 0.103 mm (100– $\bar{1}00$) \times 0.110 mm (0 $\bar{1}1$ –0 $\bar{1}\bar{1}$) \times 0.250 mm (011–0 $\bar{1}\bar{1}$).

The crystal was mounted on an Enraf-Nonius CAD-4 diffractometer and a set of 25 reflections randomly distributed in the Ewald sphere was obtained by the SEARCH procedure of the CAD-4 software. These reflections were centered in the counter and the indexing routine yielded a reduced cell of monoclinic symmetry, which was checked by means of oscillation photographs taken along the three axes. These photographs showed the expected layer-line spacings. A mirror plane was observed for oscillation along the 12.33 \AA axis, identifying this direction as the unique axis of a monoclinic cell. The Niggli matrix unambiguously indicated that no higher symmetry was present. The initial cell edges were transformed to define the conventional monoclinic cell described above. The systematic absences characteristic of space group $P2_1/c$ ($h0l$, $l \neq 2n$ and $0k0$, $k \neq 2n$) were subsequently confirmed by inspection of the complete data set.

The intensity data were collected in the θ – 2θ scan mode on a Syntex P $\bar{1}$ diffractometer. The scan range was from 1 $^{\circ}$ below $\text{K}\alpha_1$ to 1 $^{\circ}$ above $\text{K}\alpha_2$, and the scan rate varied between 1 and 24 $^{\circ} \text{min}^{-1}$. The background-time-to-scan-time ratio was 0.50. The measured sphere was limited by $2\theta_{\text{max}} = 55^{\circ}$ ($0 \leq h \leq 15$, $0 \leq k \leq 16$, $-17 \leq l \leq 14$). Three standard reflections were monitored every 47 measurements. They showed an average random fluctuation of $\pm 1.5\%$. A total of 3901 unique reflections (hkl , $hk\bar{l}$) was collected, of which 2096 reflections with $I/\sigma(I) > 3.0$ were retained for structure determination. An absorption correction was applied (Gaussian integration, grid $10 \times 10 \times 10$, transmission range 0.177–0.429). The data were finally corrected for Lorentz and polarization effects.

The structure was solved from a Patterson map, which revealed the positions of the Au and Cl atoms. The remaining non-hydrogen atoms were found from difference Fourier maps. However, since O4 and N6 differed by only one electron and they were related by a pseudo-two-fold axis through C2 and C5, care had to be taken to assign these sites to the correct atom type. Both distributions were tested by refining all non-hydrogen atoms anisotropically to convergence by full-matrix least-squares procedures. Individual weights based on counting statistics were applied. The solution retained is considered to be the correct one for the following reasons: (i) it corresponds to the relative peaks heights observed in the difference Fourier map phased on all the remaining non-hydrogen atoms (amplitude greater for O4); (ii) with this model, the thermal ellipsoids for O4 and N6 are similar to each other and comparable with those of the other atoms in the uracil ring. When O and N are interchanged, thermal motion becomes abnormally high for O and low for N; (iii) the agreement factors for the model retained are $R = \Sigma||F_o| - |F_c||/\Sigma|F_o| = 0.040$ and $R_w = [\Sigma w(|F_o| - |F_c|)^2/\Sigma w|F_o|^2]^{1/2} = 0.041$. Higher values of 0.042 and 0.043, respectively, are obtained for the alternate model.

All hydrogen atoms were visible in the difference Fourier map calculated at this stage. The presence of the N6-H proton in the map provided further support to the model accepted above. All hydrogens were fixed at idealized positions: N–H = 0.87 \AA , sp^2 hybridization; phenyl C–H = 0.95 \AA , sp^2 hybridization; methyl C–H = 0.95 \AA , sp^3 hybridization; isotropic $B = 6.5$ \AA^2 . All non-hydrogen atoms were refined anisotropically. The hydrogen parameters were not refined, but the coordinates were recalculated after each least-squares cycle. The final agreement factors were $R = 0.038$ and $R_w = 0.039$. The goodness-of-fit ratio was 1.08 for 210 parameters refined. The maximum and mean values of the shift/e.s.d. ratio in the last cycle were 0.17 and 0.03, respectively. The residuals on the final difference Fourier map were +1.3 and -1.0 e \AA^{-3} (both near Au and Cl), the general background was below $\pm 0.7 \text{ e \AA}^{-3}$.

The scattering curves for the non-hydrogen atoms were taken from Cromer and Waber [13], and those for hydrogen from Stewart *et al.* [14]. The anomalous dispersion coefficients f' and f'' were included in the structure-factor calculations for Au and Cl [15]. The final atomic coordinates and the equivalent isotropic temperature factors are listed in Table 1.

Results and Discussion

Tetrachloroauric acid reacted with the amino-azo derivative of dimethyluracil (DZCH) in alcohol, forming a red solid of composition $[\text{Au}(\text{DZC})\text{Cl}_2]$.

TABLE 1. Refined atomic coordinates ($\times 10^4$, $\times 10^5$ for Au) and equivalent isotropic temperature factors ($\times 10^3$)

Atom	x	y	z	U_{eq}
Au	12396(4)	12293(4)	4874(4)	36
Cl1	2788(3)	804(3)	2355(3)	53
Cl2	202(4)	2334(3)	1140(3)	59
Cl3	4241(3)	1910(3)	821(3)	62
O2	-3117(9)	1037(8)	-4977(8)	79
O4	598(8)	-961(7)	-3305(7)	59
N1	-1655(8)	1323(7)	-3063(7)	40
N3	-1288(9)	-11(7)	-4127(8)	43
N6	-197(9)	1616(7)	-1115(7)	42
N7	1505(8)	-34(6)	-1253(7)	33
N8	2048(8)	281(6)	-208(7)	33
C1	-2598(12)	2096(10)	-3044(11)	53
C2	-2055(12)	781(9)	-4113(10)	49
C3	-1762(16)	-577(11)	-5223(11)	76
C4	-76(11)	-302(9)	-3203(9)	44
C5	305(10)	268(8)	-2110(9)	32
C6	-529(10)	1073(8)	-2083(9)	36
C9	3347(11)	-153(9)	519(9)	37
C10	4469(12)	516(10)	1032(9)	49
C11	5718(12)	94(11)	1667(10)	57
C12	5860(12)	-1012(12)	1791(11)	66
C13	4803(13)	-1687(10)	1327(10)	54
C14	3527(11)	-1278(10)	672(9)	46

The IR spectra [7] provided some information on the coordination sphere of gold in this compound. The sharp $\nu(\text{N-H})$ band at 3342 cm^{-1} , likely due to the deprotonated 6-NH⁻ group [16], suggested that the pyrimidine derivative in $[\text{Au}(\text{DZC})\text{Cl}_2]$ was bound in the monoanionic imine form. The shift of the ligand $\nu(\text{N=N})$ band (1529 cm^{-1}) to lower frequency was indicative of gold binding to a nitrogen atom of the azo group, probably the chlorophenyl-substituted one, since the same nitrogen was found to be coordinated in the bis(1-phenylazo-2-naphtholato)M(II) complexes of Cu(II) and Ni(II) [17, 18]. In the low-frequency region, the gold(III) complex showed two new bands at 337 and 361 cm^{-1} , attributed to the Au-Cl stretching modes of a *cis* AuCl₂ unit.

The predictions are borne out by the following crystallographic work.

Crystallographic Work

X-ray diffraction shows that the crystal of $[\text{Au}(\text{DZC})\text{Cl}_2]$ contains the individual molecule shown in Fig. 1.

Interatomic distances and bond angles are provided in Tables 2 and 3. The geometry around the metal is slightly distorted square planar. Two *cis* corners are occupied by Cl ligands. The uracil derivative is coordinated via the deprotonated N6 amino group and one of the azo nitrogen atoms, thereby forming a six-membered chelate ring.

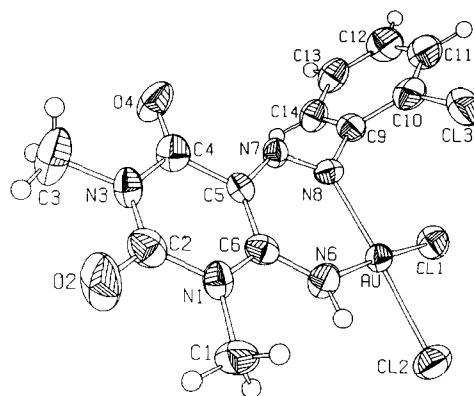


Fig. 1. ORTEP drawing of the molecule. Ellipsoids correspond to 50% probability. Hydrogens are shown as small spheres of arbitrary size.

TABLE 2. Interatomic distances and bond angles in the coordination sphere and phenyl ring

Distances (Å)			
Au-Cl1	2.275(3)	C10-C11	1.373(20)
Au-Cl2	2.300(4)	C10-C13	1.740(13)
Au-N6	1.992(9)	C11-C12	1.374(20)
Au-N8	2.029(10)	C12-C13	1.358(21)
C9-C10	1.406(18)	C13-C14	1.393(20)
C9-C14	1.402(16)		
Angles (°)			
Cl1-Au-Cl2	89.88(13)	N8-C9-C14	119.8(10)
Cl1-Au-N6	176.4(3)	C10-C9-C14	118.4(11)
Cl1-Au-N8	94.3(3)	C13-C10-C9	118.2(10)
Cl2-Au-N6	86.9(3)	C13-C10-C11	120.1(10)
Cl2-Au-N8	175.8(3)	C9-C10-C11	121.7(12)
N6-Au-N8	88.9(4)	C10-C11-C12	118.5(13)
Au-N6-C6	126.3(8)	C11-C12-C13	121.8(13)
Au-N8-N7	127.0(7)	C12-C13-C14	120.7(13)
Au-N8-C9	120.0(7)	C9-C14-C13	118.9(12)
N8-C9-C10	121.7(10)		

The Au-Cl distances (2.275(3), 2.300(4) Å) compare well with those found in similar compounds (range 2.260–2.295 Å) [11, 19–23]. The Au-N(azo) distance of 2.029(10) Å is much shorter than those observed with the 2-(phenylazo)phenyl ligand (2.17(1) Å [21], 2.140(14) Å [22]). The Au-N6 distance (1.992(9) Å) to the deprotonated amino group is also short, compared with those found in various Au-NH₃ compounds (2.01–2.04 Å) [23–25] and in the cytosine complex 2.031(16) [11].

The AuN₂Cl₂ unit is approximately planar, the largest deviation from the plane being 0.055(10) Å for N6. The mean planes through the chelate ring and the pyrimidine unit make angles of 172.6 and 163.9°, respectively, with the AuN₂Cl₂ plane. Hence, these three units define a roughly planar entity, from which only the phenyl group is excluded. The departure of

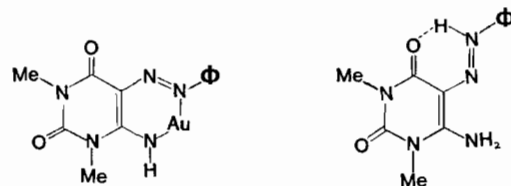
TABLE 3. Comparisons of distances and angles in uracil, the [Au(DZC)Cl₂] complex and the [DZCH₂]⁺ cation

	[Au(DZC)Cl ₂]	[DZCH ₂] ⁺ ^a	Uracil ^b
Distances (Å)			
N1–C1	1.482(18)	1.477	
N1–C2	1.407(14)	1.408	1.379
N1–C6	1.338(14)	1.351	1.380
C2–N3	1.343(17)	1.384	1.373
C2–O2	1.232(16)	1.193	1.218
N3–C3	1.457(16)	1.465	
N3–C4	1.373(16)	1.371	1.383
C4–C5	1.476(15)	1.447	1.440
C4–O4	1.199(16)	1.221	1.227
C5–C6	1.417(17)	1.433	1.338
C5–N7	1.338(15)	1.327	
C6–N6	1.332(13)	1.293	
N7–N8	1.268(11)	1.296	
N8–C9	1.433(16)	1.397	
Angles (°)			
C1–N1–C2	117.5(10)	116.7	
C1–N1–C6	120.5(10)	119.6	
C2–N1–C6	121.6(10)	123.6	121.3
N1–C2–O2	118.2(12)	121.0	123.2
N1–C2–N3	119.0(11)	117.0	114.8
N3–C2–O2	122.8(12)	122.0	122.0
C2–N3–C3	117.2(11)	118.0	
C2–N3–C4	125.2(11)	124.0	127.0
C3–N3–C4	117.6(11)	118.0	
N3–C4–O4	121.4(11)	120.2	119.8
N3–C4–C5	114.4(10)	117.1	114.7
C5–C4–O4	124.2(11)	122.6	125.4
C4–C5–C6	120.4(10)	119.9	119.2
C4–C5–N7	111.4(10)	123.8	
C6–C5–N7	128.2(10)	116.2	
N1–C6–N6	119.1(10)	120.3	
N1–C6–C5	119.3(10)	118.2	122.8
C5–C6–N6	121.6(10)	121.4	
C5–N7–N8	124.8(9)	118.8	
N7–N8–C9	112.9(9)	121.8	

^aAverage over two non-equivalent cations, $\sigma = 0.009$ Å and 0.7° , ref. 10. ^bStandard values, $\sigma = 0.002$ Å, $1-2^\circ$, ref. 27.

the angles around Au from 90° are significant, but relatively small. In particular, the N6–Au–N8 angle of $88.9(4)^\circ$ indicates that the ligand can adjust its 'bite' to maintain a normal angle at the metal. The Au–N6–C6 and Au–N8–N7 angles ($126.3(8)$ and $127.0(7)^\circ$, respectively) also correspond well with the orientation expected for the lone pairs on the donor atoms. The chelate ring is significantly puckered, perhaps to relieve tension accompanying ring closure. The distances to the mean plane are as follows: N6 $+0.171(10)$, C5 $-0.145(11)$, C6 $-0.043(12)$, N7 $+0.004(9)$, N8 $+0.112(9)$ and Au $-0.0004(5)$ Å. The angles at C5 and N7 are also severely distorted to fit the geometry of the chelate ring, as revealed by a comparison of the geometry of the present [Au-

(DZC)Cl₂] complex with the [DZCH₂]⁺ cation [7, 10] (Table 3). In both cases, the phenyl and pyrimidine groups occupy *trans* positions about the N7=N8 bond. Whereas the phenyl ring is roughly perpendicular to the C5–N7=N8–C9 plane (dihedral angle 67.1°), the pyrimidine ring is retained in this plane by Au coordination in the chelate or by intramolecular N8–H⁺...O4 hydrogen bonding in the protonated cation. Therefore, the C4=O4 bond is *syn* with respect to the N7=N8 bond in the cation, whereas the C6–N6 bond has this orientation in the complex (Scheme 1). In fact, these two conformations differ by a 180° rotation of the N7=N8–Ph group about the C5–N7 bond. The angles at C5 and C7 differ considerably in these two orientations: there is a difference of $+16.8^\circ$ between the C6–C5–N7 and C4–C5–N7 angles in the complex, becoming -7.6° in the cation (Table 3). The C5–N7–N8 angle is 11.9° greater than N7–N8–C9 in the complex, but the angle at N8 is 3° greater than the other in the cation. The presence of various ways to absorb constraints should impart great versatility to this ligand.



Scheme 1.

In presence of the electron-rich AuCl₂ unit, the bond lengths between the light atoms can be determined with only limited accuracy. Comparisons are made in Table 3 between the complex, the cation and the standard uracil moiety. On bond lengths, the differences are not highly significant. The N7–N8 distance ($1.268(11)$ Å) in the complex, comparable with that of the neutral uncoordinated 6-(*p*-hydroxyphenylazo)uracil molecule ($1.265(5)$ Å) [26], seems to be somewhat shorter than in the N8-protonated cation ($1.301(8)$ Å, $1.291(8)$ Å) [10]. Surprisingly, the C6–N6 distance is found to be longer ($1.332(13)$ Å) than in the cation ($1.293(9)$ Å) in spite of the fact that an imino resonance form in the amino-deprotonated ligand could increase double bond character between C6 and N6.

Comparison of the pyrimidine ring bonds with the standard values for uracil [27] definitely shows that the C5–C6 bond order is much reduced compared with uracil (1.338 Å) both in the complex ($1.417(17)$ Å) and in the cation ($1.433(9)$ Å). Some less dramatic changes in bond order also seem to take place in the C2–N1–C6 region, where ring angles are also affected. For instance, N1–C2–N3 is 4.2° greater here than in uracil.

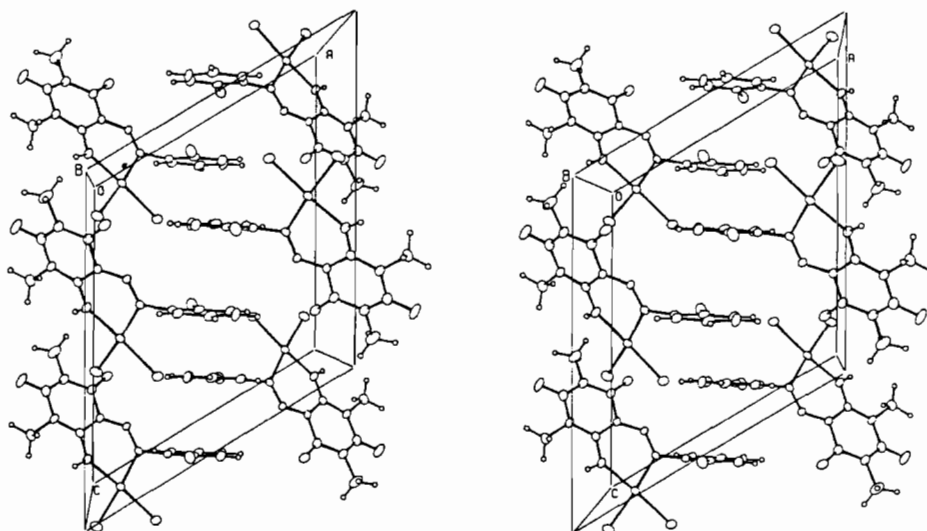


Fig. 2. Stereoview of the unit cell down the b axis. Atoms can be identified by comparison with Fig. 1. Phenyl ring stacking is clearly visible in the $x = \frac{1}{2}$ region of the unit cell.

The pyrimidine ring is planar within 2σ (0.027 Å), but most of the substituents deviate appreciably from this plane: C1 $-0.12(1)$, O2 $+0.01(1)$, C3 $-0.07(2)$, O4 $0.10(1)$, N6 $-0.01(1)$, N7 $0.08(1)$ Å. The phenyl moiety is planar within 0.7σ (0.009 Å), with significant deviations for C13 (0.023(4) Å) and N8 (0.093(9) Å). The phenyl ring is roughly perpendicular to the rest of the molecule.

A stereoview of the unit cell is provided in Fig. 2. With only N6–H as a potential donor, hydrogen bonding is not a dominant feature of molecular packing. It gives a weak N6–H...O4 interaction with one of the carbonyl oxygens in the molecule at $(\bar{x}, -\frac{1}{2} + y, -\frac{1}{2} - z)$ (N6–O4 = 3.06(1) Å, C6–N6–O4 = $108.2(7)^\circ$, N6–O4–C4 = $131.8(8)^\circ$). The coordinated Cl atoms are not involved in hydrogen bonding, participating only in normal van der Waals contacts. The roughly planar unit including the coordination plane, the chelate ring and the uracil system occupy layers in the bc face of the unit cell. A significant contribution to intermolecular forces originates from stacking of the phenyl groups, defining another layer halfway along the a axis. These rings, roughly perpendicular to the c axis, occur in pairs, separated by 3.55 Å, about crystallographic inversion centers.

Thermal Behavior

The thermogravimetric (TG) and differential scanning calorimetric (DSC) curves of DZCH and $[\text{Au}(\text{DZC})\text{Cl}_2]$ have been recorded. Both experiments show that DZCH has no definite melting point, starting to lose weight at 300 °C and continuing to decompose up to 600 °C. At that point, the sample has completely volatilized.

No weight loss is observed below 200 °C in the TG curve of $[\text{Au}(\text{DZC})\text{Cl}_2]$. At this temperature

begins a large weight-loss effect ending at 265 °C. The total loss corresponds to elimination of the chlorophenyl group and two chlorine atoms (calc. 32.2%, found 31.6%). Above 265 °C, the TG curve of $[\text{Au}(\text{DZC})\text{Cl}_2]$ shows two new weight-loss effects centered at 320 °C and $c.$ 500 °C, respectively. Both are due to pyrolytic decomposition of the pyrimidine derivative. At the end (550 °C), the weight of metallic gold obtained (34.93%) is in good agreement with the expected value (35.15%).

Supplementary Material

Lists of anisotropic temperature factor, hydrogen coordinates, least-squares plane calculations and structure factor amplitudes are available upon request from author A.L.B.

Acknowledgements

We wish to thank the Natural Sciences and Engineering Research Council of Canada for financial support to this research and the Spanish Ministry of Education and Science for a scholarship to M.Q.

References

- 1 T. M. Simon, D. H. Kunishima, G. J. Vibert and A. Lorber, *Cancer Res.*, **41** (1981) 94.
- 2 C. Dragulescu, J. Heller, A. Manzer, S. Policec, V. Topcui, M. Caalci, S. Kirschner, S. Kravitz and R. Moraski, *Coord. Chem. Conf. XVII*, **1** (1974) 99.

- 3 P. J. Sadler, M. Nasr and V. L. Narayanan, in *Platinum Coordination Complexes in Cancer Chemotherapy*, Martinus Nijhoff, Boston, MA, 1984, p. 290.
- 4 P. J. Sadler, *Struct. Bonding (Berlin)*, 29 (1976) 171.
- 5 B. Sutton, in *Platinum, Gold and other Chemotherapeutic Agents, A.C.S. Symposium Ser.*, 209 (1983) 355.
- 6 P. J. Sadler, *2nd Int. Conf. Bioinorganic Chemistry, Rev. Port. Quim.*, 27 (1985) 30.
- 7 R. Kivekäs, E. Colacio, J. Ruiz, J. D. López-González and P. León, *Inorg. Chim. Acta*, 159 (1989) 103, and refs. therein.
- 8 R. Faggiani, H. E. Howard-Lock, C. J. L. Lock and M. A. Turner, *Can. J. Chem.*, 65 (1987) 1568.
- 9 S. Hibino, *Cancer Chemother. Rep.*, 13 (1961) 141.
- 10 J. Suárez-Varela, J. P. Legros, J. Galy, E. Colacio, J. Ruiz, J. D. López-González, P. León and R. Perona, *Inorg. Chim. Acta*, 161 (1989) 199.
- 11 M. S. Holowczak, M. D. Stancel and G. B. Wong, *J. Am. Chem. Soc.*, 107 (1985) 5789.
- 12 H. Brederbeck and A. Edenhofer, *Chem. Ber.*, 66 (1955) 1306.
- 13 D. T. Cromer and J. T. Waber, *Acta Crystallogr.*, 18 (1965) 104.
- 14 R. F. Stewart, E. R. Davidson and W. T. Simpson, *J. Chem. Phys.*, 42 (1965) 3175.
- 15 D. T. Cromer, *Acta Crystallogr.*, 18 (1965) 17.
- 16 J. Ruiz Sánchez, E. Colacio Rodríguez, J. M. Salas Peregrín and M. A. Romero Molina, *J. Anal. Appl. Pyrol.*, 9 (1986) 159.
- 17 J. A. J. Jarvis, *Acta Crystallogr.*, 14 (1961) 961.
- 18 R. H. Prince and R. C. Spencer, *Inorg. Chim. Acta*, 3 (1969) 54.
- 19 P. G. Jones, J. J. Guy and G. M. Sheldrick, *Acta Crystallogr., Sect. B*, 31 (1975) 2687.
- 20 D. B. Del'Amico, F. Calderazzo, F. Marchetti and S. Merlino, *Gazz. Chim. Ital.*, 108 (1978) 627.
- 21 J. Vicente, M. T. Chicote, M. D. Bermúdez, X. Soláns and M. Font-Altaba, *J. Chem. Soc., Dalton Trans.*, (1984) 557.
- 22 J. Vicente, M. T. Chicote, M. D. Bermúdez, M. J. Sánchez-Santano, P. G. Jones, C. Fittschen and G. M. Sheldrick, *J. Organomet. Chem.*, 310 (1986) 401.
- 23 J. Strähle, J. Gelinek and M. Kölmel, *Z. Anorg. Allg. Chem.*, 456 (1979) 241.
- 24 M. Weishaupt and J. Strähle, *Z. Naturforsch., Sect. B*, 31 (1976) 554.
- 25 K. Kaas and L. H. Skibsted, *Acta Chem. Scand., Ser. A*, 39 (1985) 1.
- 26 C. L. Coulter and N. R. Cozzarelli, *Acta Crystallogr., Sect. B*, 30 (1974) 2176.
- 27 R. Taylor and O. Kennard, *J. Am. Chem. Soc.*, 104 (1982) 3209.